Journal of the Optical Society of Korea
Vol. 17, No. 2, April 2013, pp. 205-212
DOI: http://dx.doi.org/10.3807/JOSK.2013.17.2.205

Evaluation of Diffuse Reflectance in Multi-layered Tissue for High Intensity Laser Therapy

Sangkwan Lee[1] and Jong-In Youn[2]*

[1]*Department of Internal Medicine and Neuroscience, College of Oriental Medicine, Wonkwang University, Iksan 570-749, Korea*
[2]*Department of Biomedical Engineering, College of Medical Science, Catholic University of Daegu, Gyeongsan 712-702, Korea*

(Received February 1, 2013 : revised March 22, 2013 : accepted March 25, 2013)

Pain is one of the quite common symptoms in clinics and many treatment methods have been applied to relieve pain. Among the treatments, high-intensity light therapy for pain has been introduced, but this therapy has not been fully supported by confirmed efficacy due to the absence of quantitative assessments and treatment feedback data in real time. In this study, the evaluation of light distribution in tissue was performed with current high-intensity light sources quantitatively using light-tissue interaction simulations. The diffuse reflectance in tissue was generated using Monte Carlo simulation that traces photons as they undergo multiple scattering and absorption within each tissue layer (skin, fat, and muscle) and within multi-layered tissue. The results showed that the highest diffuse reflectance and the deepest penetration of tissue were achieved at λ=830 nm when compared with other wavelengths like λ=650 nm, 980 nm and 1064 nm.

Keywords : Monte Carlo simulation, Multi-layered tissue, HILT, Diffuse reflectance
OCIS codes : (170.0170) Medical optics and biotechnology; (000.1430) Biology and medicine; (120.6810) Thermal effects; (170.6510) Spectroscopy, tissue diagnostics

I. INTRODUCTION

Laser therapy has become progressively popular in the management of a wide variety of medical conditions. Laser is absorbed in the tissue, and, in turn, stimulates metabolic processes and improves pain relief and wound healing [1]. Although until now, Low Level Laser Therapy (LLLT) has been widely used with the object of removing the inflammation or the pain, LLLT was too weak to reach deep tissues, making its effectiveness very limited for most conditions [2, 3]. Many authors of clinical studies have reported the benefits of LLLT on tissue healing, but others have shown no effect [4]. The many studies on LLLT are full of conflicting reports, and much of this is caused by the lack of dosage consensus. Brosseau et al. found no effect from LLLT on ankle sprains [5]. The poor results may have been caused by insufficient irradiation, because low power did not penetrate deep tissue. Bingol et al. reported that 10 applications of LLLT for 2 weeks did not induce significant pain relief and improvements in articular function relative to the findings for a group control given a placebo [6].

High Intensity Light Therapy (HILT) for pain has been introduced but this therapy has not been fully supported by confirmed efficacy due to the absence of quantitative assessments [7]. HILT delivers high amounts of photons directly to the injured tissue, accelerating the cellular reproduction. HILT involves high-intensity laser radiation which causes minor and slow light absorption by chromophores. This absorption is obtained not with concentrated light but with diffuse light in all directions by scattering phenomenon, increasing photochemistry effects (stimulating mitochondrial oxidative reaction and adenosine triphosphate, RNA, or DNA production) and resulting in the phenomenon of photobiology effects in tissue [8]. HILT penetrates deeply into muscles, ligaments, tendons, and joints and can be employed for various indications including disorders, pain relief, and wound healing. It increases the function of local

*Corresponding author: jyoun@cu.ac.kr
Color versions of one or more of the figures in this paper are available online.

blood vessels through a process allowing oxygen and nutrient-rich blood to flow to the injured tissue area. Moreover HILT provides a comfortable feeling during the treatment, and treatment times are also significantly reduced when treating with high intensity laser [9]. HILT is more effective than conventional methods such as TENS, ultrasound therapy for pain relief. Santamato et al. evaluated the short-term effectiveness of HILT versus ultrasound therapy in the treatment of subacromial impingement syndrome (SAIS). Participants in the HILT group showed significantly greater decrease in pain than participants in the US therapy group [10]. Zati et al. evaluated the efficacy of HILT, compared with accepted therapies such as TENS and NSAIDs. HILT has proved versatility and efficacy in the treatment of many different musculoskeletal diseases and it is believed to have anti-inflammatory, anti-edema and analgesic effects [11]. Lorenzo et al. compared the effectiveness of HILT therapy (Nd:YAG laser, λ=1064nm) vs. an ultrasound technique on myofascial adductor muscles and pes anserina bursitis. Patients in the study group reported significantly more reduction in pain than with the standard ultrasound technique [12].

For laser therapy applications, it is important to know the penetration depth and the overall distribution in deep tissue depending on the laser wavelength to determine the volume of the tissue where the laser-induced photobiological reactions occur before applying laser treatments, because an insufficient treatment depth reduces the treatment efficiency, whereas an excessive depth is very likely to cause various minor effects [13]. Best et al. demonstrated treatment with positive results by high level laser therapy (λ=810 nm, 980 nm) in order to define therapeutical concepts. Patient with injury of tendon and ligaments reported positive results with functioning and pain relief [14]. Szymańska et al. observed the effect of low level laser therapy and high intensity laser therapy on endothelial cell proliferation in vitro-preliminary communication to evaluate the influence of LLLT (λ=660 nm, 670 nm, 820 nm) and HILT (λ=808 nm) on the proliferation of endothelial cells. HILT stimulated the proliferation of human umbilical vein endothelial cells (HUVEC) [15]. Fortuna et al. investigated the anti-inflammatory effect of Nd:YAG laser (λ=1064nm) in degenerative osteoarthritis. The serologic data revealed the anti-inflammatory effect with a highly significant difference between the treated group and the control group [16]. However, even though HILT has demonstrated clinical effects, it has not yet demonstrated effects according to wavelengths and differences between single layer and multi- layered tissues.

The diffuse reflectance to light transport in tissue provides an excellent estimation of depth penetration for applications in which the tissue scattering is the dominant optical interaction with light [17, 18]. The diffuse reflectance is defined as the photon probability of re-emission from the inside of an infinite turbid medium per unit surface area. The photon trajectories through the tissue form a banana shaped region with the ends at the positions of the delivery and receiving fibers [19, 20]. As the source-detector distance increases the average path length increases significantly while the average photon visit depth increases only slightly. Maximum penetration depth of light is thought to be approximately half the distance between source and detector [21, 22]. Studies have been widely performed to analyze optical propagation in various media. Farrell et al. have developed an instrument to estimate penetration depth from the spatially resolved diffuse reflectance [23]. Takatani and Graham developed a two-layer photon diffusion model that was shown to provide a good description of diffuse reflectance from intestinal tissue [24]. Kienle et al. using a two-layer diffusion approximation model showed that the derived solutions of the diffusion equation are close to the results obtained from two layer Monte Carlo simulations [25]. However, in human tissue, the propagation of light within tissue is known to be complex. Although the detected region is the same tissue type, the mean and effective penetration depths are thought to vary according to each tissue layer (skin, fat, muscle) thickness, tissue type and to the laser wavelength used. Therefore this has made it difficult to quantify these penetration depths and the distribution of light in tissue [26].

The purpose of this study is to estimate and compare between diffuse reflectance and the penetration depth in single tissue layers (skin/fat/muscle) and multi-layered tissue the dependence on different laser wavelengths using Monte Carlo simulation. This mathematical modeling may provide a better understanding of laser and tissue interaction dependence on wavelength and help to determine the optimal wavelength for effective HILT.

II. SIMULATION METHOD

The Monte Carlo simulation technique, which is based on the statistical nature of radiation interactions, has been widely applied in laser radiation transport studies [27, 28]. This mathematical modeling may provide a better understanding of the interaction between tissue and laser depending on wavelength and help to determine the effective wavelength as a function of deeper penetration in tissue. When the photon is launched, if there is a mismatched boundary at the tissue surface, then some specular reflectance will occur. The specular reflectance depends on the average refractive index and on the surface texture [26, 29]. The remaining photon weight after the specular reflection is transmitted into the tissue. The step size of each launched photon(s) and the azimuthal angle Φ are calculated based on a random sampling of the probability distribution for the photon's free path. The computer's random number generator yields a random variable from 0 to 1.

$$S = -\ln \zeta / \mu_t \tag{1}$$

$$\Phi = 2\pi\zeta \tag{2}$$

where ζ is a random number equally distributed between 0 and 1 ($0 < \zeta \leq 1$). μ_t is the extinction coefficient($\mu_t=\mu_a+\mu_s$) where μ_a is the absorption coefficient and μ_s is the scattering coefficient, and g is the anisotropy of scattering.

The photon packet loses its weight partially at the end of each step as a result of absorption. The amount of weight loss is the photon weight at the beginning of the step multiplied by (1-α), where α is the albedo $\mu_s/(\mu_a+\mu_s)$. The next event that happens to the photon packet after absorption is scattering. When an anisotropy factor (g) value is 0, indicating isotropic scattering, the cosine of the deflection angle is described as:

$$\cos\theta = 2\zeta - 1 \tag{3}$$

When an anisotropy factor (g) value is near 1, indicating anisotropic scattering, both of the cosine of the deflection angle are described as:

$$\cos\theta = \frac{1}{2g}\left(1 - g^2 - \left[\frac{1-g^2}{1-g+2g\zeta}\right]^2\right) \tag{4}$$

For the case of multi-layered tissue, during the simulation, the photon may hit a boundary between tissue layers. The photon can be either internally reflected by the boundary or it can escape as observed reflectance. Several steps are involved in the simulation when the photon hits a boundary of the layer. 1) The distance between the photon point and the boundary is calculated. 2) The next step decides whether the step size is greater than distance (between the photon point and the boundary). 3) If the photon hits a boundary, the probability of a photon being internally reflected is computed. This depends on the angle of incidence onto the boundary. If angle of incidence is larger than the critical angle, then the internal reflectance is set to 1. Otherwise is it is calculated by Fresnel's equation [27-29].

$$R(\theta_i) = \frac{1}{2}\left[\frac{\sin^2(\theta_i-\theta_t)}{\sin^2(\theta_i+\theta_t)} + \frac{\tan^2(\theta_i-\theta_t)}{\tan^2(\theta_i+\theta_t)}\right] \tag{5}$$

where θ_t is the angle of transmittance. 4) To determine whether or not the photon is reflected by the boundary or transmits into lower tissue, a random number (ζ), is generated. If $\zeta \leq R(\theta_i)$ then the photon is reflected or $\zeta > R(\theta_i)$ then the photon is transmitted [27-29].

Some of the transmitted light will re-emerge through the air-skin interface into the air. The re-emergence of light will result in the observed diffuse reflection. Their weights are accordingly scored into the diffuse reflectance or diffuse transmittance depending on where the photon packet exits from the tissue. Diffuse reflectance (J/cm^2) comprising

TABLE 1. Tissue optical properties [31-33]

		650 nm	830 nm	980 nm	1064 nm
Skin	μ_a (cm^{-1})	0.08	0.095	0.37	0.2
	μ_s (cm^{-1})	170	105	150	200
	n	1.44			
Fat	μ_a (cm^{-1})	0.116	0.083	0.123	1
	μ_s (cm^{-1})	125	112.5	105	178
	n	1.44			
Muscle	μ_a (cm^{-1})	1.03	0.3	0.53	0.5
	μ_s (cm^{-1})	88	70	58	60
	n	1.37			
	Photon #	10000			

μ_a: Absorption coefficient, μ_s: Scattering coefficient, n: refractive index

photons which enter the tissue and subsequently are scattered back through the irradiated tissue surface. The diffuse reflectance depends on the tissue scattering coefficient and scattering anisotropy, which determine the probability that a photon is backscattered by either single or multiple scattering interactions, and that it might be absorbed along its optical path within the tissue [30].

A three-dimensional model was used for the simulation consisting of three layers with almost homogeneous properties: the skin, the fat and the muscle. The thicknesses of the skin, fat and muscle layers were 1.5 mm, 3 mm and 3 mm, respectively(Fig. 1). The optical parameters of different layers corresponding to wavelengths 650 nm, 830 nm, 980 nm, and 1064 nm are presented in Table 1 [31-33]. Wavelength dependent absorption and scattering coefficients can be assigned to skin, fat and muscle, respectively. The anisotropy for skin tissue, g, defined as the mean cosine of the deflection angle due to a scattering event, has typical value (g=0.9). These optical properties of the tissues for simulation were determined on the basis of literature values [31-33]. Although a real biological tissue is never infinitely wide, it can be so treated on the condition that it is much larger than the spatial extent of the photon distribution.

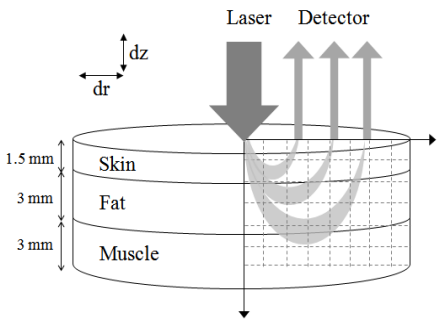

FIG. 1. Geometry for tissue modeling.

III. RESULTS AND DISCUSSION

This study investigated the penetration depth and the fluence at different wavelengths with reference to the diffuse reflectance from a single tissue layer and from multi-layered tissue irradiated by HILT. The diffuse reflectance to light transport in tissue provides an excellent estimation of depth penetration for applications in which the tissue scattering is the dominant optical interaction with light. As the scattering coefficient increases, the average photon visit depth and the average photon path length increase. As the absorption coefficient increases, the average photon path length decreases and the energy of the detected photon packets at a deep position decreases [19]. Due to strong absorption in skin, a small amount of light penetrates into muscle and light must traverse a great distance to reach the detector, and diffuse reflectance is decreased. On the other hand, if large amounts of light penetrate into muscle, light must traverse a shorter distance to reach the detector, and diffuse reflectance is increased.

Figure 2(a) shows that the results of diffuse reflectance profiles on the radius (between source and detector) and Fig. 2(b) shows that the results of laser fluence over the depth at skin tissue depending on the laser wavelength (λ =650 nm /830 nm /980 nm/1064 nm). In the skin tissue, the highest diffuse reflectance and laser fluence were achieved at λ=1064 nm, followed by, in order, λ=650 nm, λ=830 nm and λ=980 nm. Light absorption is influenced by both the wavelength and the composition of the tissue. Because melanin and water have a wavelength-dependent absorption coefficient, the distribution of these components (melanin, water) influences the optical properties of skin [34]. The light absorption by water in tissue is higher at λ =1064 nm than at visible wavelengths [35]. Thereby, the high diffuse reflectance, which was also found at λ=1064 nm with short radius, may arise from high absorption by water in the skin tissue. λ=650 nm wavelength which has high absorption of chromophores such as melanin, determines a small penetration depth of light into the skin tissue and correspondingly, larger diffuse reflectance than other wavelengths. On the other hand, chromophores contained in the epidermis absorb less in the near IR range (λ=830 nm, 980 nm, and 1064 nm) than in the visible range (λ =650 nm) of the spectrum. Since the absorption at λ=830 and λ=980 nm in skin is lower than that of other wavelengths, it appears that both λ=830 and λ=980 nm have small diffuse reflectance in short radius.

Figure 3 shows that the results of diffuse reflectance profiles(a) and laser fluence(b) at fat tissue depending on the laser wavelength (λ=650 nm /830 nm /980 nm/1064 nm). In the fat tissue, the highest diffuse reflectance and laser fluence were achieved at λ=1064 nm followed by, in order, λ=650 nm, λ=830 nm and λ=980 nm. Because the absorption spectrum of lipids is similar to that of water, λ =1064 nm is strongly absorbed by fat and water. The highest diffuse reflectance was achieved at λ=1064 nm with short radius. However, the diffuse reflectance at λ =1064 nm was decreased dramatically with increasing radius.

Figure 4 shows the results of diffuse reflectance profiles(a) and laser fluence(b) at muscle tissue depending on the laser wavelength (λ=650 nm/830 nm/980 nm/1064 nm). In the muscle tissue, the highest diffuse reflectance and laser fluence were achieved at λ=650 nm followed by, in order, λ=830 nm, λ=1064 nm, and λ=980 nm. The main chromophores in optical spectra of muscle are hemoglobin, myoglobin, and the cytochromes [36]. λ=650 nm is strongly absorbed by deoxy-hemoglobin and λ=830 nm is absorbed by oxy-hemoglobin [37]. Thereby the diffuse reflectance is increased at λ=650 nm and λ=830 nm in the surface of muscle.

The diffuse reflectance and laser fluence at each tissue layer presented similar tendencies according to the results in Figs. 2-4. In skin and fat tissue, λ=1064 nm shows the high laser fluence by the strong absorption in the surface of each tissue. On the other hand, λ=650 nm and λ=830

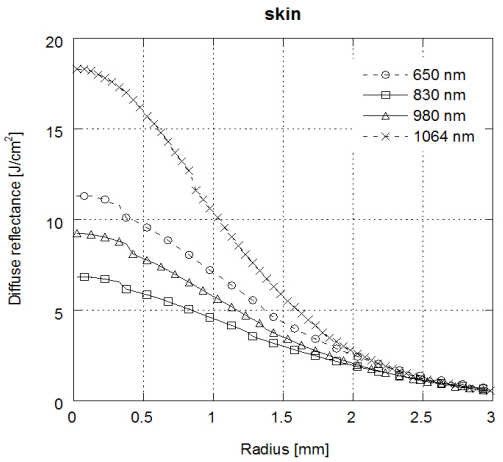

(a)

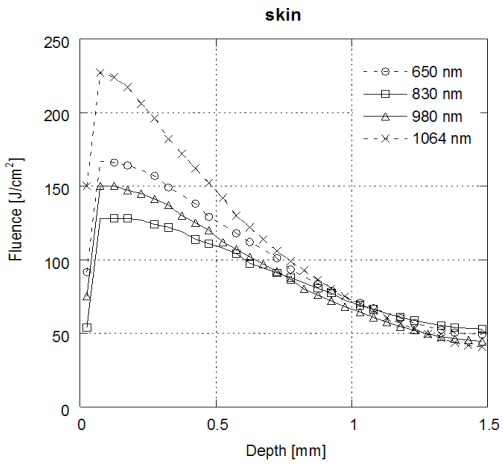

(b)

FIG. 2. (a) Diffuse reflectance as a function of the distance from the laser to the detector and (b) fluence at skin tissue as a function of depth with different laser wavelengths.

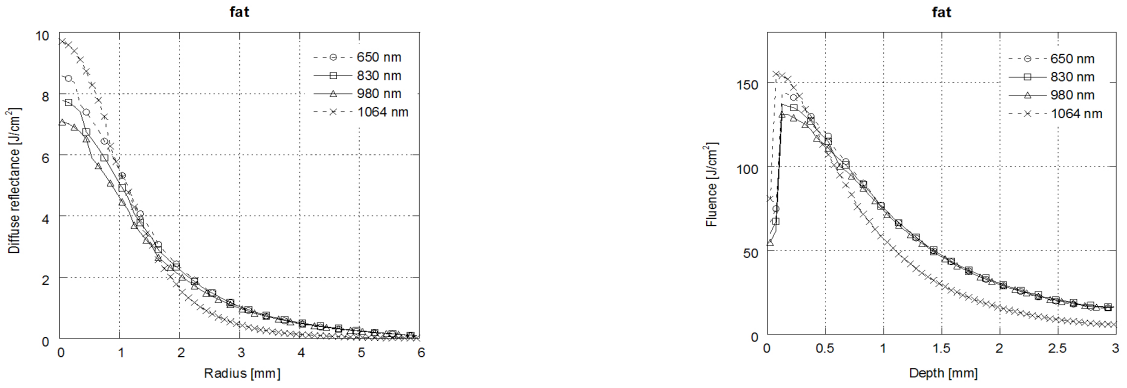

(a) (b)

FIG. 3. (a) Diffuse reflectance as a function of the distance from the laser to the detector and (b) fluence at fat tissue as a function of depth with different laser wavelengths.

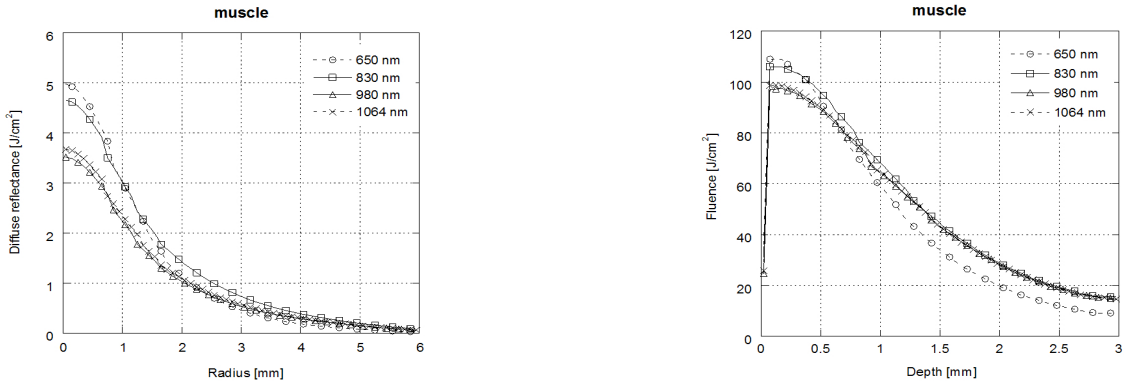

(a) (b)

FIG. 4. (a) Diffuse reflectance as a function of the distance from the laser to the detector and (b) fluence at muscle tissue as a function of depth with different laser wavelengths.

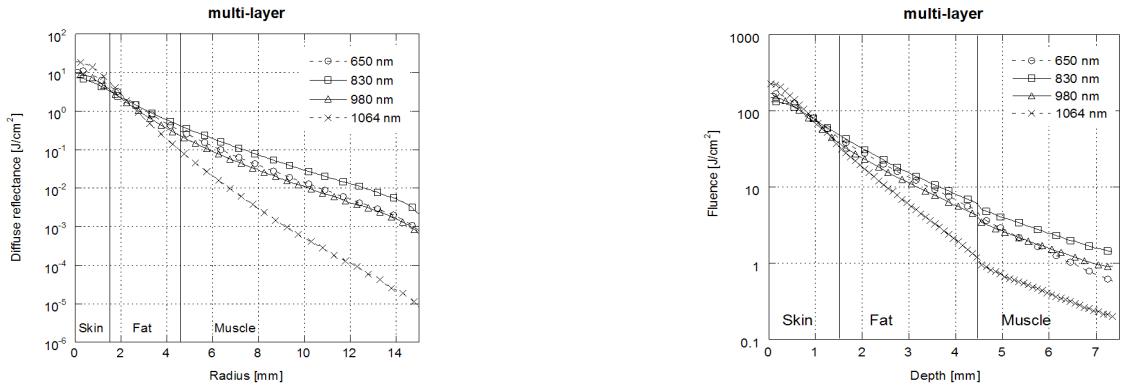

(a) (b)

FIG. 5. (a) Diffuse reflectance and (b) fluence in multi-layered tissue depending on the laser wavelengths.

nm show the high laser fluence by the strong absorption in the surface of muscle tissue. It is expected that the basis-dependent results that the diffuse reflectance can be used to provide an accurate prediction of the laser fluence in the tissue.

Figure 5 shows the results of laser diffuse reflectance and laser fluence in multi-layered tissue depending on the laser wavelength. Diffuse reflectance and laser fluence in multi- layered tissue was significantly different compared with those in each layer (skin/fat/muscle). Weersink et al. reported that a layer structure in the tissue, with each layer having different optical properties, affects the way in

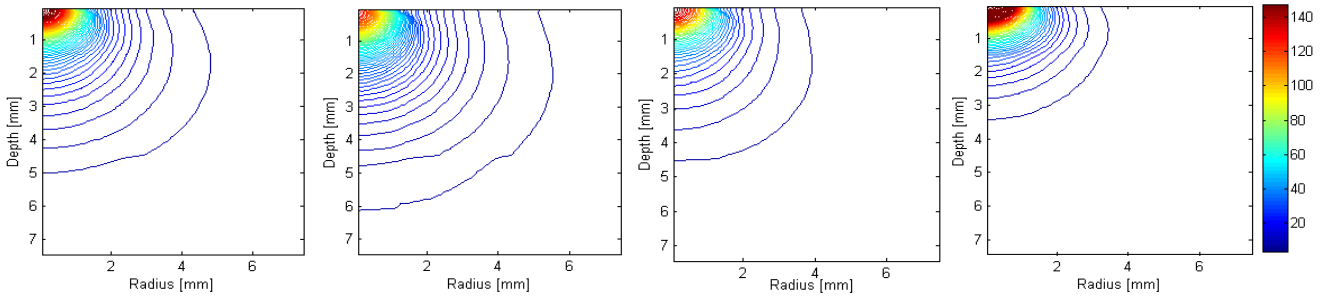

FIG. 6. Two dimensional distribution of fluence in multi-layered tissue depending on the laser wavelength (a) 650 nm, (b) 830 nm, (c) 980 nm, (d) 1064 nm.

which the light is distributed on the surface [32]. The muscle tissue may change both diffuse reflectance and laser fluence, as a result of which the spectral composition of light emerging from the upper tissue (skin and fat) is changed. Unlike Monte Carlo simulation results in each layer, due to high absorption in skin and fat, the penetration depth of incident photons into tissue is small at the λ=1064 nm. The highest diffuse reflectance was achieved at λ=1064 nm wavelength in short radius (<3 mm), but decreased dramatically with increasing radius. On the other hands, the diffuse reflectance at λ=830 nm was higher than λ=1064 nm with increasing radius (<3mm). Thereby λ=830 nm laser that traveled through deep tissue result in a larger diffuse reflectance.

Figure 6 shows the results of two dimensional distribution of laser fluence in multi-layered tissue. Since high absorption in skin and fat at λ=1064 nm, the incident photons only reach up to the fat tissue. On the other hand, λ=650 nm and 980 nm are penetrated deeper tissue than λ =1064 nm and reached up to surface of muscle. However, λ=830 nm penetrated deeply and spread widely into muscle tissue. This can be explained by the fact that λ =650 nm, λ=980 nm, and λ=1064 nm have a property of high absorption in skin and fat. This means that a skin or fat layer prevents a substantial amount of light passing through to the muscle tissue at λ=650 nm and λ=830 nm, and λ=1064 nm wavelength. Thereby, light is not going through the deep tissue and is localized in the surface. λ =830 nm has a property of lower absorption in skin and fat than for other wavelengths, resulting in more delivery up to deep tissue. It appears that λ=830 nm laser penetrates the muscle tissue. With these results, the clinician can select the optimal light wavelength delivered to skin so that the laser fluence is delivered to the target region. The most commonly used laser for HILT is an Nd:YAG laser with a wavelength of λ=1064 nm. However, these results suggest that λ=830 nm penetrate deeply into the muscle tissue enough to reach half the distance between the light and the detector. For the future experiments, it is necessary to investigate the temperature and light distributions in tissue phantom and ex vivo tissues for the validation of the simulation results in this study.

IV. CONCLUSION

In this study, we have demonstrated that the diffuse reflectance in multi-layered tissue depends strongly on wavelength, and we have evaluated the light distribution in tissue with high intensity laser quantitatively using Monte Carlo simulations. The simulation was performed with each layer tissue (skin, fat, muscle) and multi-layered tissue, and compared the diffuse reflectance for tissue according to the distance (between source and detector) and laser fluence distribution over the depth. In multi-layered tissue of Monte Carlo simulation results, λ=830 nm, λ=980 nm have larger diffuse reflectance, and spread laser fluence in deeper tissue. λ=650 nm, λ=1064 nm, have the smallest diffuse reflectance, and localized laser fluence in surface tissue. Therefore, λ=830 nm and λ=980 nm could help to treatment tissue in deeper region, and λ=650 nm, λ=1064 nm could help to treatment tissue in surface region. During laser therapy, laser power is controlled according to diffusion reflectance intensity for each person for reaching optimally tissue injuries.

ACKNOWLEDGMENT

This research was supported by Basic Science Research Program through the National Research Foundation of Korea (NRF) funded by the Ministry of Education, Science and Technology (2010-0008977, 2010-0029468).

REFERENCES

1. D. Hawkins, N. Houreld, and H. Abrahamse, "Low level laser therapy(LLLT) as an effective therapeutic modality for delayed wound healing," Ann. N. Y. Acad. Sci. **1056**, 486-493 (2005).
2. M. Malm and T. Lundeberg, "Effect of low power gallium arsenide laser on healing of venous ulcers," Scand. J. Plast.

Reconstr. Hand Surg. **25**, 249-251 (1991).
3. T. Lundeberg and J. Zhou, "Low power laser irradiation does not affect the generation of signals in a sensory receptor," Am. J. Chinese Med. **16**, 87-91 (1988).
4. J. T. Hopkins, T. A. McLoda, J. G. Seegmiller, and G. D. Baxter, "Low-level laser therapy facilitates superficial wound healing in humans: a triple-blind, sham-controlled study," J. Athl. Train. **39**, 223-229 (2004).
5. L. Brosseau, V. Welch, G. Wells, R. deBie, A. Gam, K. Harman, M. Morin, B. Shea, and P. Tugwell, "Low level laser therapy (classes I, II and III) for the treatment of osteoarthritis," The Cochrane Library, Issue 2, Oxford: Update Software (2000).
6. U. Bingol, L. Altan, and M. Yurtkuran, "Low power laser treatment for shoulder pain," Photomed. Laser Surg. **23**, 459-464 (2005).
7. M. S. Baggish, "High-power-density carbon dioxide laser therapy for early cervical neoplasia," Am. J. Obstet. Gynecol. **136**, 117-125 (1980).
8. P. Fiore, F. Panza, G. Cassatella, A. Russo, V. Frisardi, V. Solfrizzi, M. Ranieri, L. Di Teo, and A. Santamato, "Short-term effects of high-intensity laser therapy versus ultrasound therapy in the treatment of low back pain: a randomized controlled trial," Eur J Phys Rehabil Med. **47**, 367-373 (2011).
9. A. Zati, E. S. Degli, and T. W. Bilotta, "II laser CO2: effetti analgesici e psicologici in uno studio controllato," Laser & Technology **7**, 723730 (1997).
10. A. Santamato, V. Solfrizzi, F. Panza, G. Tondi, V. Frisardi, B. G. Leggin, M. Ranieri, and P. Fiore, "Short-term effects of high-intensity laser therapy versus ultrasound therapy in the treatment of people with subacromial Impingement syndrome: a randomized clinical trial," Phys. Ther. **89**, 643-652 (2009).
11. A. Zati, D. Fortuna, A. Valent, M. V. Filippi, and T. W. Bilotta, "High intensity laser therapy (HILT) versus TENS and NSAIDs in low back pain: clinical study," Proc. SPIE **5610**, 277-283 (2004).
12. L. D. Lorenzo, A. M. Forte, F. Forte, A. Corbisiero, V. D. Franco, and D. Sicari, "Pes anserinus bursitis and thight adductors' myofascial pain in adult non professional sportsman after a knee strain: the effect of laser HILT versus ultrasound during early rehabilitation," EUR MED PHYS **45** (2009).
13. L. E. Dolotov, Y. P. Sinichkin, V. V. Tuchin, G. B. Al'tshuler, and I. V. Yaroslavskii, "Specific features of diffuse reflection of human face skin for laser and non-laser sources of visible and near-IR light," Quantum Electron. **41**, 329 (2011).
14. N. Best, S. Derlien, and U. C. Smolenski, "High level laser therapy at patients with musculoskeletal disorders. A treatment with 120 patients," Physikalische Medizin, Rehabilitationsmedizin, Kurortmedizin A **20**, 262-265 (2010).
15. J. Szymańska, M. Lukowicz, K. Góralczyk, M. Weber-Zimmermann, and D. Rość, "Effect of low level laser therapy and high intensity laser therapy on endothelial cell proliferation in vitro-preliminary communication," Medical and Biological Sciences **22**, 79-84 (2008).
16. D. Fortuna, G. Rossi, T. W. Bilotta, A. Zati, I. Cardillo, A. Venturini, S. Pinna, C. Serra, and L. Masotti, "Nd:YAG laser in experimentally induced chronic degenerative osteoarthritis in broiler chickens: pilot study," Proc. SPIE **4903**, 77 (2002).
17. A. J. Welch, G. Yoon, and M. J. C. van Gemert, "Practical models for light distribution in laser-irradiated tissue," Lasers Surg. **6**, 488-493 (1987).
18. S. Takatani and M. D. Graham, "Theoretical analysis of diffuse reflectance from a two-layer tissue model," IEEE Trans. Biomed. Eng. **26**, 656-664 (1979).
19. I. Kenji, M. Katsuhiko, A. Hidenobu, H. Koji, N. Tetsu, and Y. Yukio, "Monte Carlo simulation of near infrared reflectance spectroscopy in the wavelength range from 1000 nm to 1900 nm," Optical Review **10**, 600-606 (2003).
20. A. A. Stratonnikov and V. B. Loschenov, "Evaluation of blood oxygen saturation *in vivo* from diffuse reflectance spectra," J. Biomed. Opt. **6**, 457-467 (2001).
21. P. van der Zee, M. Cope, S. R. Arrdge, M. Essenpreis, L. A. Potter, A. D. Edwards, J. S. Wyatt, D. C. McCormick, S. C. Roth, and E. O. Reynolds, "Experimentally measured optical pathlength for the adult head, calf, and forearm and the head of the newborn infant as a function of interoptode spacing," Adv. Exp. Med. Biol. **316**, 143-153 (1992).
22. G. Zonios and A. Dimou, "Modeling diffuse reflectance from semi-infinite turbid media: application to the study of skin optical properties," Opt. Express **14**, 8661-8674 (2006).
23. C. M. Gardner, S. L. Jacques, and A. J. Welch, "Light transport in tissue: accurate expressions for one-dimensional fluence rate and escape function based upon Monte Carlo simulation," Lasers Surg. Med. **18**, 129-138 (1996).
24. J. M. Schmitt, G. X. Zhou, E. C. Walker, and R. T. Wall, "Multilayer model of photon diffusion in skin," J. Opt. Soc. Am. A **7**, 2141-2153 (1990).
25. A. Kienle, M. S. Patterson, N. Dognitz, R. Bays, G. Wagnieres and H. van den Bergh, "Noninvasive determination of the optical properties of two-layered turbid media," Appl. Opt. **37**, 779-791 (1998).
26. M. C. van Beekvelt, M. S. Borghuis, B. G. van Engelen, R. A. Wevers, and W. N. Colier, "Adipose tissue thickness affects *in vivo* quantitative near-IR spectroscopy in human skeletal muscle," Clinical Science **101**, 21-28 (2001).
27. J. S. Dam, P. E. Andersen, T. Dalgaard, and P. E. Fabricius, "Determination of tissue optical properties from diffuse reflectance profiles by multivariate calibration," Appl. Opt. **37**, 772-778 (1998).
28. L. Wang, S. L. Jacques, and L. Zheng, "MCML-Monte Carlo modeling of light transport in multi-layered tissues," Computer Methods and Programs in Biomedicine **47**, 131-146 (1995).
29. T. J. Farrell, M. S. Patterson, and B. C. Wilson, "A diffusion theory model of spatially resolved, steady-state diffuse reflectance for the non-invasive determination of tissue optical properties *in vivo*," Med. Phys. **19**, 879-888 (1992).
30. H. Zeng, C. MacAulay, C. Palcic, and D. I. McLean, "A computerized autofluorescence and diffuse reflectance spectro-analyser system for *in vivo* skin studies," Phys. Med Biol. **38**, 231-240 (1993).
31. Y. Yang, O. Soyemi, P. J. Scott, M. R. Landry, S. M. Lee, L. Stroud, and B. R. Soller, "Quantitative measurement of muscle hemoglobin oxygenation using near-infrared spectroscopy with correction for the influence of a subcutaneous fat layer," Opt. Express **15**, 13715-13730 (2007).

32. G. R. Schweinsberger, C. M. Cilip, S. R. Trammell, H. Cherukuri, and N. M. Fried, "Noninvasive laser coagulation of the human vas deferens: optical and thermal simulations," Lasers Surg. Med. **43**, 443-449 (2011).
33. G. Vargas, E. K. Chan, J. K. Barton, H. G. Rylander III, and A. J. Welch, "Use of an agent to reduce scattering in skin," Laser Surg. Med. **24**, 133-141 (1999).
34. N. Bogduk and A. Marsland, "The cervical zygapophysial joints as a source of neck pain," Spine **13**, 610-617 (1988).
35. R. A. Weersink, J. E. Hayward, K. R. Diamond, and M. S. Patterson, "Accuracy of noninvasive *in vivo* measurements of photosensitizer uptake based on a diffusion model of reflectance spectroscopy," Photochem. Photobiol. **66**, 326-35 (1997).
36. R. Weersink and R. White, and L. Lilge, "Light dosimetry for low-level laser therapy: accounting for differences in tissue and depth," Proc. SPIE **6428**, 642803 (2007).
37. D. A. Boas, A. M. Dale, and M. A. Francechini, "Diffuse optical imaging of brain activation: approaches to optimizing image sensitivity, resolution, and accuracy," NeuroImage **23**, 275-288 (2004).